IEEE Photonics Journal
An IEEE Photonics Society Publication

Multi-Orbital-Angular-Momentum Multi-Ring Fiber for High-Density Space-Division Multiplexing

Volume 5, Number 5, October 2013

Shuhui Li
Jian Wang, Member, IEEE

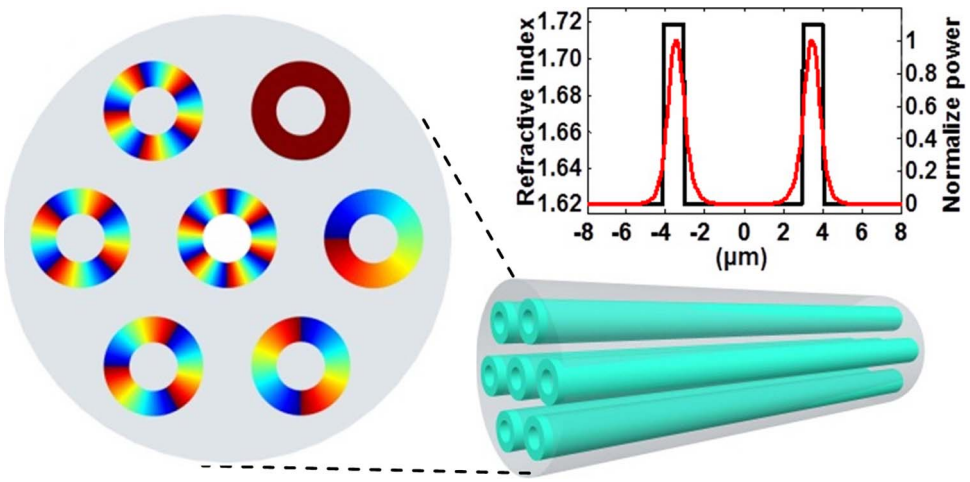

DOI: 10.1109/JPHOT.2013.2272778
1943-0655 © 2013 IEEE

Multi-Orbital-Angular-Momentum Multi-Ring Fiber for High-Density Space-Division Multiplexing

Shuhui Li and Jian Wang, *Member, IEEE*

Wuhan National Laboratory for Optoelectronics, Huazhong University of Science and Technology, Wuhan 430074, China

DOI: 10.1109/JPHOT.2013.2272778
1943-0655 ©2013 IEEE

Manuscript received May 22, 2013; revised June 27, 2013; accepted June 28, 2013. Date of publication July 22, 2013; date of current version September 23, 2013. This work was supported by the National Natural Science Foundation of China (NSFC) under grants 11274131, 61222502, and L1222026, the National Basic Research Program of China (973 Program) under grant 2014CB340004, and the Fundamental Research Funds for the Central Universities (HUST) under grant CXY13Q023. Corresponding author: J. Wang (e-mail: jwang@hust.edu.cn).

Abstract: A compact low-crosstalk multi-ring fiber transmitting multiple orbital angular momentum (OAM) modes is presented. The multi-OAM-mode multi-ring fiber (MOMRF) consists of 7 rings, each supporting 22 modes with 18 OAM ones (i.e., 154 channels in total), which can be used for high-density space-division multiplexing. The employed high-contrast-index ring structure benefits tight light confinement and large effective refractive index difference of different OAM modes ($> 10^{-4}$), featuring both low-level inter-ring crosstalk (< -30 dB for a 100-km-long fiber) and intermode crosstalk over a wide wavelength range (1520–1580 nm). The designed MOMRF is also compatible with wavelength-division multiplexing technique (e.g., 75 ITU-grid wavelengths from 1520.25 to 1579.52 nm with 100-GHz spacing) and advanced multilevel amplitude/phase modulation formats (e.g., 16-ary quadrature amplitude modulation), which might be used to achieve petabit-per-second total transmission capacity and hundred bits-per-second-per-hertz aggregate spectral efficiency.

Index Terms: Orbital angular momentum (OAM), multi-orbital-angular-momentum multi-ring fiber (MOMRF), space-division multiplexing (SDM), optical fiber communications.

1. Introduction

"Twisted" light beams, having helical phase fronts along the direction of propagation, carry orbital angular momentum (OAM) which is a fundamental physical quantity of light [1]. OAM-carrying twisted light beams, also called OAM beams, have been widely used in a variety of interesting applications ranging from optical manipulation to quantum information processing [2]–[6]. Very recently, OAM beams have also attracted much attention for increasing transmission capacity and spectral efficiency in both free-space and fiber optical communication systems [7]–[10]. Generally speaking, OAM beams with different charge numbers (i.e. different values of orbital angular momentum) are inherently orthogonal with each other. Hence, it is expected that OAM beams can be employed as information carriers for spatial mode-division multiplexing, providing alternative option to tackle the capacity crunch beyond existing multiplexing techniques.

To some extent, OAM multiplexing is similar to the well-known space-division multiplexing (SDM) with multi-core fiber (MCF) and few-mode fiber (FMF) in fiber optical transmission systems [11], [12]. In general, linearly polarized (LP) modes are adopted in FMF and the number of LP modes to

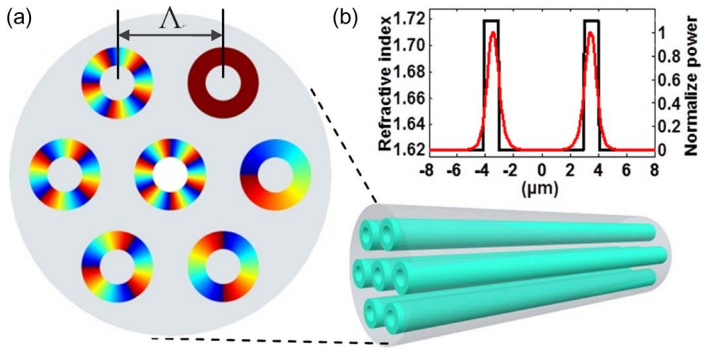

Fig. 1. (a) 3D structure and cross-section of multi-OAM-mode multi-ring fiber (MOMRF). (b) Index profile of single ring (black) and mode profile of TE_{01} mode (red) in the ring.

be multiplexed is limited to a small value to relieve inter-mode crosstalk and simplify processing complexity (e.g. multiple-input multiple-output (MIMO)). In order to develop fiber multi-mode communications using OAM, several challenges should be considered: i) special fiber design supporting OAM modes; ii) simultaneous transmission of multiple OAM modes with low-level inter-mode crosstalk; iii) compatible with existing multiplexing techniques. Fiber-based OAM generation and transmission using specially designed high-index ring structure have been reported [8], [13]–[15]. Another laudable goal would be to further optimize the fiber structure to transmit multiple OAM modes without impacting on each other. Additionally, in view of recent works of few-mode multi-core fiber [16], it would be also valuable to combine fiber OAM multiplexing and multi-core-like structure for high-density SDM applications.

In this paper, we propose a simple multi-OAM-mode multi-ring fiber (MOMRF) for SDM. The large difference of effective refractive index of fiber eigenmodes $(>10^{-4})$ in each ring are assumed to benefit negligible inter-mode crosstalk. Moreover, the high-contrast-index ring structure enables a much lower-level inter-ring crosstalk (<-30 dB for a 100-km long fiber). The designed fiber contains 7 rings with each ring supporting 22 modes (18 OAM ones), i.e. 154 channels in total, which can be used for high-density SDM.

2. Design of Multi-OAM-Mode Multi-Ring Fiber

Fig. 1(a) illustrates the 3D structure and cross-section of the designed MOMRF in which 7 identical high-index rings are arranged hexagonally. The ring-to-ring distance Λ and the cladding diameter of the MOMRF are 30 μm and 125 μm, respectively. The materials used in the MOMRF are (1) ring: Schott SF4 with $n_r = 1.72$, (2) cladding: Schott SF2 with $n_c = 1.62$ (1550 nm). Practical fabrication of special fiber using similar type of materials has been achieved [17], [18]. Fig. 1(a) also depicts phase distributions of different OAM modes (phase of one mode in each ring is plotted as an example). Fig. 1(b) shows the refractive index profile (black curve) of a single ring with the inner radius r_1 of 3 μm and outer radius r_2 of 4 μm. The calculated mode profile (red curve) of TE_{01} mode guided by the ring structure is also shown in Fig. 1(b).

Note that crosstalk is one of the most important parameters characterizing the performance of SDM applications. Generally speaking, there are three types of crosstalk in the MOMRF: (1) inter-mode crosstalk of different order OAM modes in the same ring; (2) inter-ring crosstalk of the same order OAM mode in different rings; (3) crosstalk of different order OAM modes in different rings which can be ignored when both inter-mode and inter-ring crosstalks are negligible. A reasonable way to design and optimize the proposed MOMRF is expected to study and minimize the inter-mode crosstalk and inter-ring crosstalk.

3. Results and Discussions

We optimize the fiber design using the aforementioned geometry parameters to effectively suppress both inter-mode and inter-ring crosstalks. We first characterize in detail the guided modes

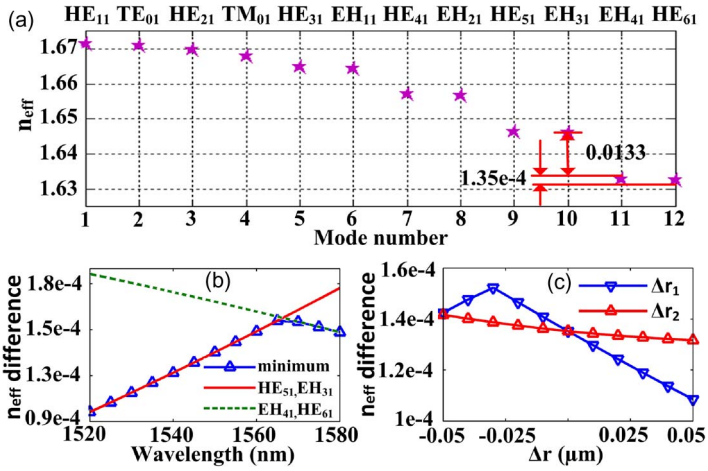

Fig. 2. (a) Effective refractive index (n_{eff}) of all fiber eigenmodes in a single ring. (b) Minimum n_{eff} difference versus wavelength. (c) Minimum n_{eff} difference versus variation of inner (r_1) or outer (r_2) ring radius.

in each single ring of the proposed MOMRF and show their properties in terms of effective refractive index (n_{eff}), wavelength dependence, and phase distributions. Remarkably, not conventional optical fiber but a high-contrast-index ring fiber is used to support OAM modes as such structure can increase the n_{eff} difference of fiber eigenmodes [19]. It is believed that large n_{eff} difference can benefit reduced inter-mode crosstalk.

Fig. 2(a) shows n_{eff} of all fiber eigenmodes at 1550 nm in each ring calculated by finite-element method. Note that each HE_{mn} or EH_{mn} also contains even and odd modes, hence 22 fiber eigenmodes are supported in a single ring of the designed MOMRF. The maximum n_{eff} difference can be as high as 0.0133 between EH_{31} and EH_{41} modes, and even the minimum n_{eff} difference can reach 1.35×10^{-4} between EH_{41} and HE_{61} modes. With these fiber eigenmodes (i.e. TE_{01}, TM_{01}, HE_{mn}, EH_{mn}), one can obtain 22 modes with 18 OAM ones which are combined by even and odd modes of HE_{mn} or EH_{mn} modes with a $\pm\pi/2$ phase shift [20], i.e. $HE_{mn}^{even} \pm i \times HE_{mn}^{odd}$, $EH_{mn}^{even} \pm i \times EH_{mn}^{odd}$. The corresponding topological charge number of OAM mode is $\pm(m-1)$ for $HE_{mn}^{even} \pm i \times HE_{mn}^{odd}$ while $\pm(m+1)$ for $EH_{mn}^{even} \pm i \times EH_{mn}^{odd}$, respectively. In particular, the large n_{eff} difference $(>10^{-4})$ among all the supported fiber eigenmodes are assumed to benefit negligible inter-mode crosstalk [8], [16], [19]. For instance, in a recent OAM-based mode-division multiplexing over a 1.1-km fiber, different modes transmitted along the fiber separately with negligible inter-mode crosstalk owing to the large effective refractive index difference $(\sim 10^{-4})$, which succeeded in the long-length mode-division multiplexing system without using any multiple-input multiple-output (MIMO) processing. Additionally, compared to the well-known FMF supporting only few number of LP modes, the optimized design of high-contrast-index ring fiber can transmit 22 modes (18 OAM ones) simultaneously with low-level inter-mode crosstalk. We also study the dependence of minimum n_{eff} difference on the wavelength and fabrication tolerance (i.e. variation of inner or outer ring radius). As shown in Fig. 2(b), the minimum n_{eff} difference almost remains above 10^{-4} within a wavelength range from 1520 to 1580 nm which covers the whole C band and enters into the S and L bands. The wavelength-dependent n_{eff} difference between HE_{51} and EH_{31} as well as between EH_{41} and HE_{61} is also plotted for reference. Actually, Fig. 2(b) indicates that the designed ring structure can be compatible with existing wavelength-division multiplexing (WDM) technique. Within 1520 to 1580 nm, multiple wavelengths (e.g. 75 ITU-grid wavelengths from 1520.25 to 1579.52 nm with 100-GHz spacing) each having 22 modes with low-level inter-mode crosstalk can be multiplexed together to increase the transmission capacity. As shown in Fig. 2(c), the minimum n_{eff} difference keeps above 10^{-4} with varied inner (r_1: 2.95 to 3.05 μm) or outer (r_2: 3.95 to 4.05 μm) ring radius, featuring favorable fabrication tolerance.

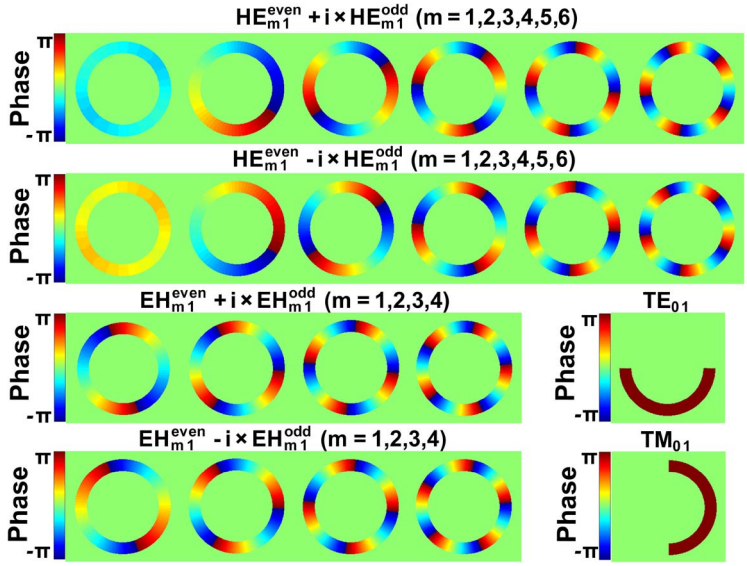

Fig. 3. Spatial phase distributions of the x-component electric field of 22 modes (18 OAM ones) in MOMRF.

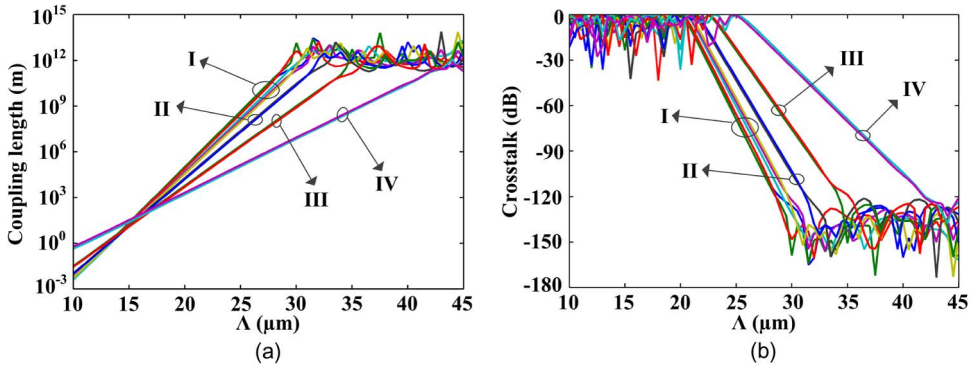

Fig. 4. (a) Coupling length of OAM modes in adjacent rings versus Λ. (b) Crosstalk of OAM modes in adjacent rings versus Λ (propagation length: 100 km).

Fig. 3 depicts calculated spatial phase distributions of the x-component electric field of all 22 modes including 18 OAM ones, i.e. TE_{01}, TM_{01}, $HE_{mn}^{even} \pm i \times HE_{mn}^{odd}$ $(m = 1, 2, 3, 4, 5, 6)$, $EH_{mn}^{even} \pm i \times EH_{mn}^{odd}$ $(m = 1, 2, 3, 4)$. It is noted that TE_{01} and TM_{01} feature binary phase distributions of 0 and π. $HE_{11}^{even} + i \times HE_{11}^{odd}$ and $HE_{11}^{even} - i \times HE_{11}^{odd}$, show almost constant phase distributions. In particular, one can clearly see the spiral phase distributions of 18 OAM modes with non-zero topological charge numbers, i.e. $HE_{mn}^{even} \pm i \times HE_{mn}^{odd}$ $(m = 2, 3, 4, 5, 6)$ and $EH_{mn}^{even} \pm i \times EH_{mn}^{odd}$ $(m = 1, 2, 3, 4)$. Similar to few modes in FMF, those 22 modes are orthogonal with each other and can be used for spatial mode-division multiplexing.

After enabling low-level inter-mode crosstalk for multi-OAM modes in each single ring, we further comprehensively analyze the inter-ring crosstalk for the multi-ring structure. In order to determine the Λ necessary for negligible inter-ring crosstalk, we study the power transfer between two adjacent rings. The normalized power transfer between two identical rings is given by $\sin^2(\pi z/(2L_c))$ with z being the propagation length and L_c being the coupling length [21]. The coupled-mode theory method [22], which has the ability to accurately evaluate ultra-long coupling length $(10^{10}$ m), is adopted to calculate the L_c. Fig. 4(a) shows L_c of different OAM modes in adjacent rings as a function

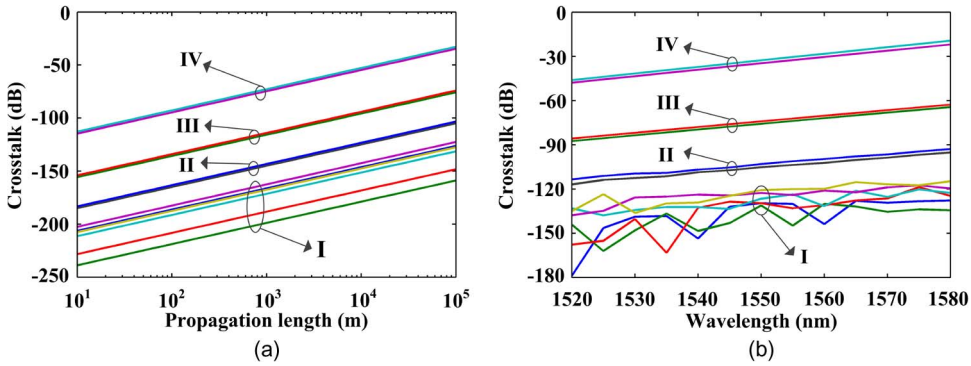

Fig. 5. (a) Crosstalk of OAM modes in adjacent rings versus propagation length. (b) Crosstalk of OAM modes in adjacent rings versus wavelength (propagation length: 100 km).

of Λ. For simple description, we divide 22 modes including 18 OAM ones into four groups, i.e. group I: TE_{01}, TM_{01}, $HE_{11}^{even} + i \times HE_{11}^{odd}$, $HE_{11}^{even} - i \times HE_{11}^{odd}$, and HE_{21}, HE_{31}, EH_{41} related OAM modes; group II: HE_{41} and EH_{21} related OAM modes; group III: HE_{51} and EH_{31} related OAM modes; group IV: EH_{41} and HE_{61} related OAM modes. As shown in Fig. 4(a), it is found that L_c increases with the increase of Λ. This is easy to understand as large separation between adjacent rings can reduce mode overlap and power transfer between adjacent rings, resulting in a long L_c. One may note the oscillation effect in Fig. 4(a), which can be ascribed to the fact that the adopted coupled-mode theory features its precision limitation when calculating the coupling length longer than 10^{10} m. However, 10^{10} m coupling length is longer enough to ensure a very low inter-ring crosstalk. When Λ is 30 μm and the wavelength is 1550 nm, for the first group I, L_c has an order of 10^{10} m; while for the last group IV, L_c has an order of 10^6 m. Such phenomenon can be explained with the fact that lower-order modes are confined more tightly than higher-order ones in the ring.

When the propagation length z is 100 km, Fig. 4(b) plots the inter-ring crosstalk of 22 modes (18 OAM ones) in adjacent rings as a function of Λ. One can clearly see the decrease of inter-ring crosstalk with the increase of Λ. For small values of Λ, the relative small L_c according to Fig. 4(a) causes rapid oscillation of crosstalk defined by $10\log_{10}(\sin^2(\pi z/(2L_c)))$. For large values of Λ, the oscillation of crosstalk is due to limited calculation accuracy of Lc $(10^{10}$ m$)$ by coupled-mode theory. When Λ is fixed at 30 μm, the inter-ring crosstalk in adjacent rings for group I is lower than -100 dB, and the maximum inter-ring crosstalk in adjacent rings is about -32.8 dB for EH_{41} related OAM mode in group IV. Compared with a conventional homogeneous single mode MCF which needs to set the core-to-core distance around 70 μm to obtain a -30 dB inter-core crosstalk for a propagation length of 100 km [21], the compact size of the designed MOMRF structure can be contributed to the high-contrast-index ring configuration and resultant tight mode confinement.

To further assess the performance of the designed MOMRF, we also calculate the inter-ring crosstalk for varied propagation length and wavelength. Fig. 5(a) shows inter-ring crosstalk of OAM modes in adjacent rings as a function of the propagation length. For a 10 km propagation length, the inter-ring crosstalk in adjacent rings is less than -90 dB for OAM modes in groups I, II and III while less than -50 dB for OAM modes in group IV. Lower inter-ring crosstalk can be clearly seen in Fig. 5(a) for shorter propagation length. The low-level inter-ring crosstalk of MOMRF indicates potential use in practical applications, especially suitable for short-distance optical fiber communications (e.g. optical access networks). Even for a 100 km propagation length, the inter-ring crosstalk in adjacent rings is still less than -50 dB for OAM modes in groups I, II and III while less than -30 dB for OAM modes in group IV. Fig. 5(b) shows inter-ring crosstalk of OAM modes in adjacent rings as a function of wavelength under a propagation length of 100 km. Within a wide wavelength range from 1520 to 1580 nm, the inter-ring crosstalk in adjacent rings is less than -60 dB for OAM modes in groups I, II and III while less than -20 dB for OAM modes in group IV. Hence, the MOMRF is also compatible with WDM technique.

The high-contrast-index ring structure with specific types of glass (Schott SF4 and SF2) benefits tight light confinement and large effective refractive index difference of different OAM modes, featuring both low-level inter-ring crosstalk and inter-mode crosstalk in the designed MOMRF. However, the design may pay the cost of relatively large loss. On one hand, it might be practical to use the designed fiber in short-distance applications (1 m $\sim$ 1 km). Under such short distance, the inter-ring and inter-mode crosstalk can be even smaller. On the other hand, the proposed MOMRF design is not limited to these specific materials. Low loss materials might be employed to effectively reduce the propagation loss [8].

Using the designed MOMRF with both negligible inter-ring and inter-mode crosstalk within a wide wavelength range (1520 to 1580 nm), it might be possible to simultaneously transmit 11550 channels (7 rings $\times$ 22 modes $\times$75 ITU-grid wavelengths from 1520.25 to 1579.52 nm with 100-GHz spacing) with negligible inter-channel crosstalk, which could increase 11550 times total transmission capacity and 154 times aggregate spectral efficiency compared with a single channel transmission. That is, when using 42.8-Gbaud/s 16-ary quadrature amplitude modulation (16-QAM) signal for each channel [7], 1.98-Pbit/s total transmission capacity and 492.8-bit/s/Hz aggregate spectral efficiency might be available.

4. Conclusion

In summary, we have designed a compact low-crosstalk MOMRF featuring multiple spatial rings and multiple OAM modes in each ring for high-density SDM. It is also compatible with existing WDM technique and advanced multi-level amplitude/phase modulation formats, holding great potential to enable Pbit/s transmission capacity and hundreds bit/s/Hz spectral efficiency. With future improvement, a comprehensive design (materials, geometric parameters) might be considered to further optimize the proposed MOMRF having more rings and each ring supporting more OAM modes over a wider wavelength range (whole C + L bands) with negligible inter-mode and inter-ring crosstalks and low propagation loss.

References

[1] L. Allen, M. W. Beijersbergen, R. J. C. Spreeuw, and J. P. Woerdman, "Orbital angular momentum of light and the transformation of Laguerre-Gaussian laser modes," *Phys. Rev. A*, vol. 45, no. 11, pp. 8185–8189, Jun. 1992.
[2] A. M. Yao and M. J. Padgett, "Orbital angular momentum: Origins, behavior and applications," *Adv. Opt. Photon.*, vol. 3, no. 2, pp. 161–204, 2011.
[3] S. Franke-Arnold, L. Allen, and M. Padgett, "Advances in optical angular momentum," *Laser Photon. Rev.*, vol. 2, no. 4, pp. 299–313, 2008.
[4] M. Padgett and R. Bowman, "Tweezers with a twist," *Nature Photon.*, vol. 5, no. 6, pp. 343–348, 2011.
[5] S. Bernet, A. Jesacher, S. Frhapter, C. Maurer, and M. Ritsch-Marte, "Quantitative imaging of complex samples by spiral phase contrast microscopy," *Opt. Exp.*, vol. 14, no. 9, pp. 3792–3805, May 2006.
[6] J. T. Barreiro, T.-C. Wei, and P. G. Kwiat, "Beating the channel capacity limit for linear photonic superdense coding," *Nature Phys.*, vol. 4, no. 4, pp. 282–286, Apr. 2008.
[7] J. Wang, J.-Y. Yang, I. M. Fazal, N. Ahmed, Y. Yan, H. Huang, Y. X. Ren, Y. Yue, S. Dolinar, M. Tur, and A. E. Willner, "Terabit free-space data transmission employing orbital angular momentum multiplexing," *Nature Photon.*, vol. 6, no. 7, pp. 488–496, Jul. 2012.
[8] N. Bozinovic, Y. Yue, Y. Ren, M. Tur, P. Kristensen, A. E. Willner, and S. Ramachandran, "Orbital angular momentum (OAM) based mode division multiplexing (MDM) over a Km-length fiber," presented at the European Conf. Exhibition Optical Communication, Amsterdam, Netherlands, Sep.16–20, 2012, Paper Th.3.C.6.
[9] F. Tamburini, E. Mari, A. Sponselli, B. Thid, A. Bianchini, and F. Romanato, "Encoding many channels on the same frequency through radio vorticity: First experimental test," *New J. Phys.*, vol. 14, p. 033001, Mar. 2012.
[10] P. Boffi, P. Martelli, A. Gatto, and M. Martinelli, "Optical vortices: An innovative approach to increase spectral efficiency by fiber mode-division multiplexing," in *Proc. SPIE*, 2013, vol. 8647, p. 864705.
[11] B. Zhu, T. F. Taunay, M. Fishteyn, X. Liu, S. Chandrasekhar, M. F. Yan, J. M. Fini, E. M. Monberg, and F. V. Dimarcello, "112-Tb/s space-division multiplexed DWDM transmission with 14-b/s/Hz aggregate spectral efficiency over a 76.8-km seven-core fiber," *Opt. Exp.*, vol. 19, no. 17, pp. 16665–16671, Aug. 2011.
[12] R. Ryf, S. Randel, A. H. Gnauck, C. Bolle, A. Sierra, S. Mumtaz, M. Esmaeelpour, E. C. Burrows, R.-J. Essiambre, J. Winzer, D. W. Peckham, A. H. McCurdy, and R. Lingle, "Mode-division multiplexing over 96 km of few-mode fiber using coherent 6$\times$6 MIMO processing," *J. Lightw. Technol.*, vol. 30, no. 4, pp. 521–531, Feb. 2012.
[13] Y. Yan, J. Wang, L. Zhang, J. Y. Yang, I. M. Fazal, N. Ahmed, B. Shamee, A. E. Willner, K. Birnbaum, and S. Dolinar, "Fiber coupler for generating orbital angular momentum modes," *Opt. Lett.*, vol. 37, no. 16, pp. 4269–4271, Nov. 2011.

[14] Y. Yan, L. Zhang, J. Wang, J.-Y. Yang, I. M. Fazal, N. Ahmed, A. E. Willner, and S. J. Dolinar, "Fiber structure to convert a Gaussian beam to higher order optical orbital angular momentum modes," *Opt. Lett.*, vol. 37, no. 16, pp. 3294–3296, Aug. 2012.
[15] Y. Yue, Y. Yan, N. Ahmed, J.-Y. Yang, L. Zhang, Y. Ren, H. Huang, K. M. Birnbaum, B. I. Erkmen, S. Dolinar, and A. E. Willner, "Mode properties and propagation effects of optical orbital angular momentum (OAM) modes in a ring fiber," *IEEE Photon. J.*, vol. 4, no. 2, pp. 535–543, Apr. 2012.
[16] C. Xia, R. Amezcua-Correa, N. Bai, E. Antonio-Lopez, D. May-Arriojo, A. Schulzgen, M. Richardson, J. Liñares, C. Montero, E. Mateo, X. Zhou, and G. Li, "Hole-assisted few-mode multi-core fiber for high-density space-division multiplexing," presented at the IEEE Photon. Soc. Summer Top. Meet., Seattle, WA, USA, 2012, Paper TuC4.2.
[17] X. Feng, F. Poletti, A. Camerlingo, F. Parmigiani, P. Horak, P. Petropoulos, W. H. Loh, and D. J. Richardson, "Dispersion-shifted all-solid high index-contrast microstructured optical fiber for nonlinear applications at 1.55 micron," *Opt. Exp.*, vol. 17, no. 22, pp. 20249–20255, Oct. 2009.
[18] F. Poletti, X. Feng, G. M. Ponzo, M. N. Petrovich, W. H. Loh, and D. J. Richardson, "All-solid highly nonlinear single mode fibers with a tailored dispersion profile," *Opt. Exp.*, vol. 19, no. 1, pp. 66–80, Jan. 2011.
[19] S. Ramachandran, P. Kristen, and M. F. Yan, "Generation and propagation of radially polarized beams in optical fibers," *Opt. Lett.*, vol. 34, no. 16, pp. 2525–2527, Aug. 2009.
[20] P. Z. Dashti, F. Alhassen, and H. P. Lee, "Observation of orbital angular momentum transfer between acoustic and optical vortices in optical fiber," *Phys. Rev. Lett.*, vol. 96, no. 4, p. 043604, Mar. 2006.
[21] M. Koshiba, K. Saitoh, and Y. Kokubun, "Heterogeneous multi-core fibers: Proposal and design principle," *IEICE Electron. Exp.*, vol. 6, no. 2, pp. 98–103, Jan. 2009.
[22] N. Mothe and P. D. Bin, "Numerical analysis of directional coupling in dual-core microstructured optical fibers," *Opt. Exp.*, vol. 17, no. 18, pp. 15778–15789, Aug. 2009.